This is an open access article published under an ACS AuthorChoice License, which permits copying and redistribution of the article or any adaptations for non-commercial purposes.

ACS OMEGA

Article

Cite This: ACS Omega 2018, 3, 2390−2395

Highly Structured Polyvinyl Alcohol Porous Carriers: Tuning Inherent Stability and Release Kinetics in Water

Juan Manuel Sonego,[†] Johanna M. Flórez-Castillo,[‡] and Matías Jobbágy*[,†]

[†]Instituto de Química Física de Materiales, Medio Ambiente y Energía—INQUIMAE, Universidad de Buenos Aires, Ciudad Universitaria Pabellón 2 (C1428EHA), Buenos Aires, Argentina

[‡]Grupo de investigación en Bioquímica y Microbiología—GIBIM, Universidad Industrial de Santander, Carrera 27 Calle 9, Bucaramanga, Santander 680002, Colombia

Supporting Information

ABSTRACT: Polyvinyl alcohol (PVA) porous carriers were prepared by means of ice templating of aqueous solutions containing of 90 kD and/or 16 kD PVA. The carriers were loaded with traces of a colored probe (methyl orange) to screen their release properties, once immersed in water. The carriers prepared from solutions containing 90 kD and 16 kD PVA resulted in intimate polymer mixtures, exhibiting physical properties that stand in between those of the bare 90 kD or 16 kD PVA end members. The freezing protocols employed were adapted to prepare carriers textured in the form of either monolithic scaffolds (directional constant freezing rate) or millimetric pellets (flash-freeze). Monolithic carriers remain stable in aqueous solution, and the probe release is governed by a swelling−diffusion mechanism. The kinetics of probe release can be tuned from minutes to hours by either increasing the total PVA content or the 90 kD-to-16 kD PVA ratio in the parent solution. In contrast, pellets (millimetric carriers) immersed in water release the probe on the scale of minutes, irrespective of the PVA content or composition. However, the PVA content and the 90 kD-to-16 kD PVA ratio dramatically affect the stability of the carriers. Depending on the formulation, these small carriers can develop swelling, erosion, or eventually massive dissolution.

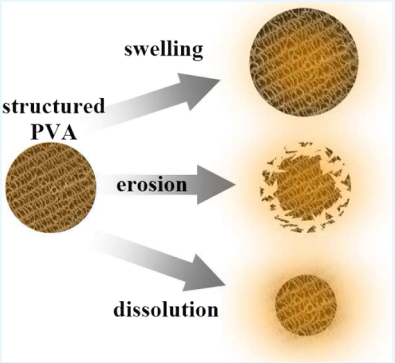

INTRODUCTION

Materials science is permanently inspired by the requirements of cutting-edge biomedical challenges. Tissue engineering, in particular, demands smarter 3D scaffolds that are able to satisfy multiple requirements in parallel, such as cell adhesion and guidance, tuned drug release, and scaffold dissolution/biosorption.[1,2] To ensure their proper performance, their texture must be defined as an interconnected pore network that guarantees an adequate mass transport with the surrounding physiological media.[2−6] In recent years, novel functional scaffolds[7] and hydrogels based on a well-established biocompatible polymer such as polyvinyl alcohol (PVA in the following) were prepared by freezing/thawing methods.[8−10] More recently, their controlled structuration by means of the ice-templating method, either from aqueous solutions or hydrogels, resulted in oriented hierarchically textured biomaterials.[11] The versatility of this method lies in the possibility of tuning the resulting scaffold texture by several physiochemical and/or chemical parameters, such as the solvent composition, the solute nature and concentration, the freezing rate, and the temperature gradient. The method was also employed in the structuration of mixtures of building blocks, including liposomes[12] or micelles[24] combined with silica polymers and nanoparticles[7] or even highly bimodal micro-/nanoparticle suspensions,[25] that can effectively coalesce within a common and well-interdispersed solid phase, after the solvent solidification. Scaffolds with controlled pore texture (size, shape, distribution, and orientation) can be obtained, even in the form of large macroscopic robust pieces.[6,11]

In the case of PVA-based scaffolds, several variables effectively tune the texture, including the polymer mass fraction in the parent solution, the average PVA molecular weight, and the freezing rate. On this basis, diverse functional PVA scaffolds, loaded with antibiotic agents[13] or living cells,[14] were created. Diverse approaches were reported for drug loading, ranging from the inclusion of micro-/nanocrystal dispersed within the pores[15] or as intimate mixtures with the scaffold polymer.[16] In the first case, drug release kinetics is mainly governed by the crystal dissolution rate. In the second case, it is controlled by the scaffold stability (swelling/erosion) and transport properties. However, in the latter case, if the mass fraction of the loaded drug is significant with respect to that of the host polymer, swelling and dissolution of the whole scaffold can be severely modified with respect to the inherent values.[16] To overcome this uncertain scenario, the present study explores the release properties of several PVA scaffolds loaded with a negligible mass fraction of dye molecules to minimize any effect of the probe on the porous texture of PVA and its inherent

Received: December 8, 2017
Accepted: February 14, 2018
Published: February 27, 2018

© 2018 American Chemical Society

DOI: 10.1021/acsomega.7b01961
ACS Omega 2018, 3, 2390−2395

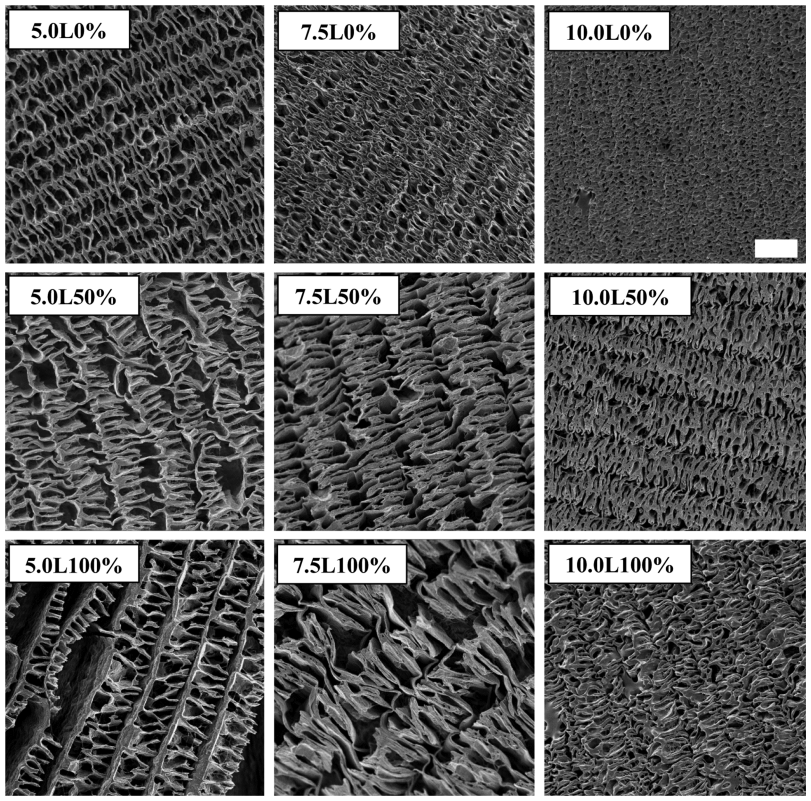

Figure 1. Field emission scanning electron microscopy (FESEM) images of PVA scaffolds frozen at 5.5 mm min^{-1}. Scale bar represents 5 μm for all images.

stability in aqueous solution. To this aim, a family of PVA scaffolds was structured by means of ice templating; scaffolds were prepared employing aqueous solutions of PVA of two different molecular weights (16 or 90 kD) as well as their binary mixtures, as an extra preparative resource to tune the inherent stability and release properties.

RESULTS AND DISCUSSION

It is known that freezing structuring processes follow several common trends, ruled by the physics of phase segregation, irrespective of the nature of the solvent and solute.[17] Ice formation drives the segregation of every solute or colloid originally dispersed in the aqueous phase toward zones in which the ice is absent, giving rise to a hierarchical assembly defined by walls, fibers, or bicontinuous arrays of matter surrounding empty areas where the ice resided before sublimation, resulting in an organized 3D scaffold. However, the existence of peculiar behaviors of each formulation imposes a careful experimental textural screening.[10,18] In the present case, as a first step, solutions containing increasing amounts of PVA were submitted to ice templating. In addition, each sample was prepared employing PVA of 16 and 90 kD and a mixture (50 m/m %) of them. All samples maintained the shape of the container in which the parent solutions were confined prior to ice templating. Figure 1 presents the micrographs revealing the texture of a series of samples prepared under representative conditions, ranging from 5 to 10% in total PVA content, employing pure 90 or 16 kD PVA as well as the binary mixture. Most of the samples can be interpreted in terms of main parallel PVA walls, periodically connected by perpendicular bridges resulting from dendritic growth of ice.[19]

A closer view of the wall texture revealed an additional level of porosity with dimensions ranging from 50 to 300 nm (see Figure S1). For a given PVA total content, more opened structures resulted from polymer with lower (16 kD or L) average molecular weights. In the case of sample 5.0L100%, the dendritic bridges cannot effectively coalesce with the nearby main walls, resulting in a discontinuous multilayered structure. In contrast, bridges and walls of sample 10.0L0% are fused enough to be almost indistinguishable, resulting in a more intricate texture. In general terms, an increment in the total PVA content in the parent solution reflected a significant contraction of pore sizes, from the range of microns to a sub-micrometric level (sample 10.0L0%). This tendency was also observed when PVA average molecular weight increases. For any set of samples with a given total PVA content, the binary 16−90 kD 50% mixtures denote an intermediate behavior with respect to the bare end members. For a given PVA formulation (0, 50, or 100%), samples with a total PVA content of 7.5 w/v % show an intermediate behavior between the behaviors of 5.0 and 10 w/v %.

No attempts to quantify these tendencies were performed on the present set of samples because the whole PVA scaffold suffered massive contractions (up to one-third of the parent freeze volume) depending on the formulation, creating severe artifacts to properly analyze the pore size (see Figure S2). It was previously reported that textural inhomogeneities can be present in the periphery of the samples (skin effect) prepared under identical conditions.[13] However, scanning electron microscopy (SEM) inspection of the present samples revealed a homogeneous texture that reaches the external surface parallel to the freezing direction, even for samples frozen at high rates. The lack of the so-called skin effect observed for related

DOI: 10.1021/acsomega.7b01961
ACS Omega 2018, 3, 2390−2395

systems[13] can be explained in terms of occurrence of an ice crust externally developed around the mold before immersion, driven by ambient moisture condensation/solidification. This external ice shell seems to allow a better heat transfer once immersed in the liquid N_2 bath, preventing the development of a texture gradient or skin (Figure 2).

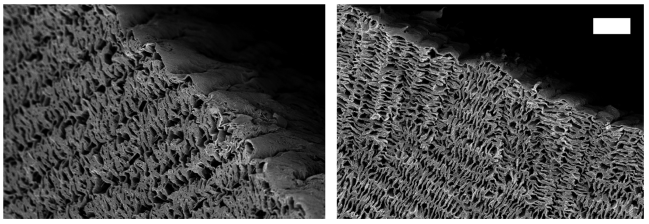

Figure 2. FESEM images of sample 7.5L50% frozen at 5 mm min^{-1} (left) and 8 mm min^{-1} (right). Scale bar represents 10 μm for both images.

To gain insights about the nature of the employed PVA combinations on a molecular scale, representative MO-free samples of 5.0 w/v % were inspected by both powder X-ray diffraction (PXRD) and differential scanning calorimetry (DSC). The former revealed the inherent broad signals of solid PVA, irrespective of the polymer molecular weight of the sample or the freezing conditions (see Figure S3). All samples revealed a DSC trace consisting of two main thermal endothermic events (see Figure 3) developed along the 460–505 K range, which can be assigned to fusion steps of different regions of the sample. Most of the previous reports describe a single asymmetric signal in this range, probably due to the faster heating rates employed therein (10–20 K min^{-1}). However, it was recently reported that textural effects and analysis conditions can lead to more complex thermal signals.[20] Beyond this, the sample 5.0L50% exhibits an intermediate behavior with respect to the end members, suggesting the intimate mixture of both kinds of PVA at a molecular level. The high degree of mixture observed herein is in line with certain recent findings that demonstrate the ability of the ice-templating method to drive the homogeneous assembly of highly heterogeneous precursor systems.[12]

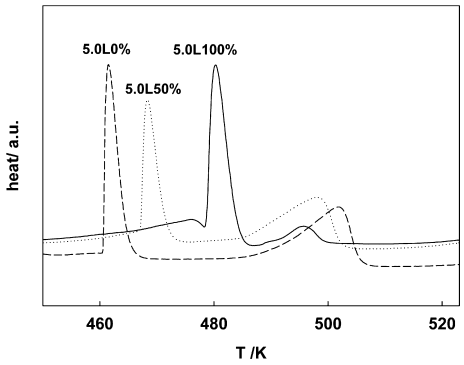

Figure 3. DSC trace for samples prepared with 5 m/v % PVA of 16 kD (5.0L100%) and 90 kD (5.0L0%) average molecular weights and the binary mixture (5.0L50%), recorded at 5 K min^{-1} under a N_2 atmosphere.

Release properties of PVA samples loaded with methyl orange probe were recorded in water at 298 K; the amount of released probe was quantified by means of UV–vis absorption at suitable time lapses. The release behavior was parameterized on the basis of the Korsmeyer–Peppas[21,22] model; cumulative release profiles were parameterized with the following expression:

$$M_t/M_\infty = kt^n \quad (1)$$

where M_t is the amount of drug permeated at time t; M_∞ is the amount of drug at infinite time; M_t/M_∞ is the fraction of permeated drug (typically obtained from M_t/M_∞ values lower than 0.6); k is a kinetic constant; and n is a release exponent that depends on the sample geometry and the hydration behavior. In contrast with related systems, no lag time associated with the swelling and plasticization of the polymeric matrix was observed.[23−25] For samples prepared with total PVA contents equal to or higher than 5 w/v %, the release profiles can be properly described, up to a 70% cumulative release, employing an exponent of $n = 0.50 \pm 0.03$ that stands compatible with an intermediate film/cylinder geometry under the Fickian regime. The release profiles of samples of increasing PVA mass fractions and their correspondent fitted curves are presented in Figure 4.

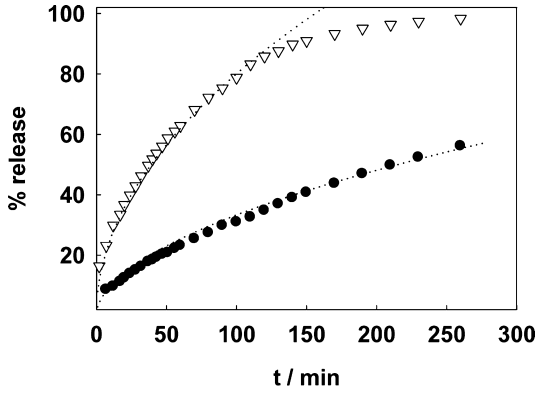

Figure 4. Cumulative release (expressed in percentage) as a function of time of samples 5.0L25% (empty triangles) and 7.5L25% (filled circles), frozen at 8 mm min^{-1}. The dotted lines represent the optimized fittings based on the Korsmeyer–Peppas model.

Samples formulated with total contents of PVA of 2.5 w/v % released the probe on the scale of tens of minutes; the obtained release profiles were noisy and difficult to fit, irrespective of the PVA nature. Then, the approximate time required to reach a release of 50%, t_{50}, was adopted as the release parameter to define the behavior of this set of samples. A comprehensive screening of release properties as a function of PVA formulation was performed on the basis of t_{50} values. The behaviors of the samples prepared with a given freezing rate, three total PVA contents (2.5, 5.0, and 7.5 w/v %), and increasing 16-to-90 kD ratios are summarized in Figure 5. In general terms, a net effect of both variables can be noticed; the release kinetics for samples ranging from 5.0 to 7.5 w/v % is clearly affected by the average molecular weight, decaying the t_{50} values to a half when 16 kD PVA is employed instead of 90 kD PVA. However, this tendency is not strictly proportional to the average molecular weight and depends also on the total PVA content. For total contents of PVA of 2.5 w/v %, the release is extremely fast, with t_{50} values centered at 13 ± 4 min, irrespective of the PVA molecular weight. Along the explored range of formulations, the release kinetics can be tuned in more than an order of magnitude. Finally, a set of samples of 5.0 w/v % PVA content

DOI: 10.1021/acsomega.7b01961
ACS Omega 2018, 3, 2390–2395

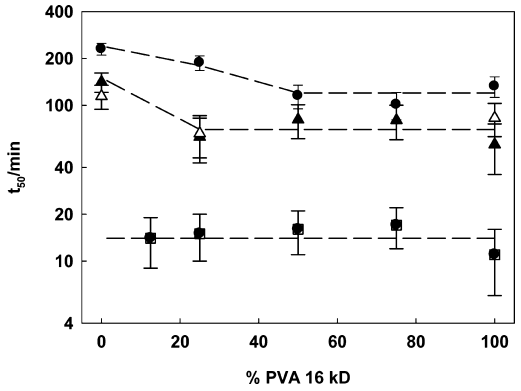

Figure 5. Dependence of t_{50} as a function of PVA 16 kD mass fraction for PVA total content of 7.5% (●), 5.0% (▲), and 2.5% (■), frozen at 8 mm min^{-1}. Samples of 5.0% content were also frozen at 5.5 mm min^{-1} (Δ).

were also prepared employing a faster freezing rate, revealing that the effect of this variable on the release is not significant (see Figure 5). The marked similarity of PXRD patterns and water stability of monolithic samples suggests a similar degree of polymer entanglement. Then, the texture of macropores seems to be the main variable that limits the probes release kinetics.

Once established the behavior of monolithic PVA carriers, an additional set of samples was prepared with similar PVA formulations in the form of small pellets (see Experimental Section for detailed procedure). This protocol allows an extremely fast freezing rate or a limiting case that illustrates up to which extent this variable can affect the final properties of PVA carriers. Once frozen, representative samples were fractured before being submitted to freeze-drying and finally inspected by FESEM; micrographs are depicted in Figure 6. In general, the porous structure remained notably disordered compared to those of the monolithic counterparts, irrespective of the employed PVA. Only the capsules of the 7.5L0% composition achieved a defined porosity, aligned with the radial freezing gradient employed. Samples with a PVA total content lower than 7.5 w/v % suffered a severe net contraction with respect to the original drop diameter.

In contrast with the monolithic carriers, pellets resulted in fast release characterized by an almost constant t_{50} value of 15 ± 7 min (see Figure S4), independently of the PVA average molecular weight or the total PVA content. However, despite this constancy, very different behaviors were observed concerning the integrity of the PVA carriers in aqueous media. In general, once a pellet is immersed in water, the probe can be released through the diffusion of a stable swelled (hydrated) PVA carrier (Scheme 1, upper path), as is the case of monolithic carriers. However, if the PVA matrix is unstable, it can be disrupted into small fragments through an erosion path that also drives release (Scheme 1, middle path). Eventually, in the case of very unstable PVA carriers, massive dissolution prevails (Scheme 1, lower path) over the aforementioned paths.

In the present case, samples with a PVA content of 2.5 w/v % resulted in massive disruption of the carrier; for the highest molecular weight, a constant scattering signal evidenced the instantaneous presence of undissolved PVA fragments in suspension, denoting a fast erosion-driven mechanism (see Scheme 1). Samples rich in 16 kD PVA resulted in negligible scattering, indicating the prevalence of dissolution. Samples

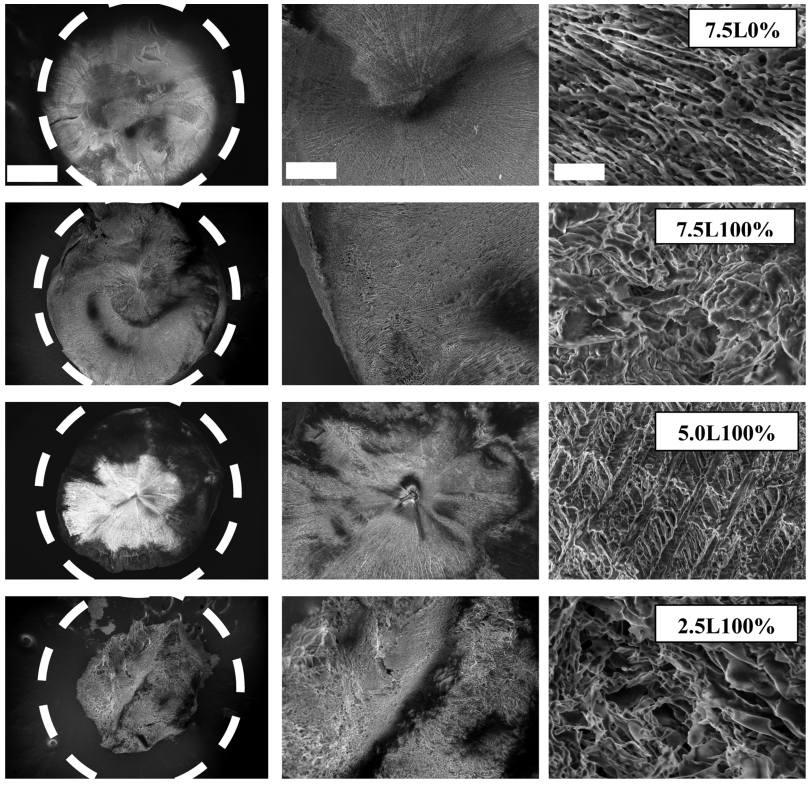

Figure 6. FESEM images of small carriers (flash-frozen) of compositions 7.5L0%, 7.5L100%, 5L100, and 25L100. Scale bars represent 0.5 mm (left row), 100 μm (central row), and 2 μm (right row). The dashed circumferences are an indicative reference of the parent drop diameter.

DOI: 10.1021/acsomega.7b01961
ACS Omega 2018, 3, 2390−2395

Scheme 1. Release Mechanisms of PVA Carriers Immersed in Water: Swelling Diffusion (Upper Path), Disruption by Erosion (Middle Path), and Massive Dissolution (Lower Path)

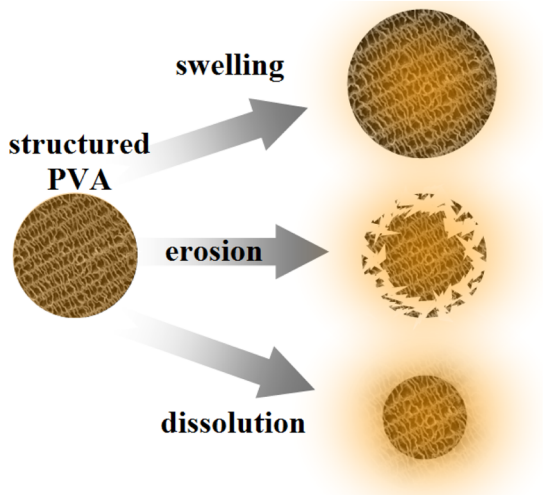

with a total PVA content of 5.0 w/v % evidenced an increasing scattering signal along the experiment, irrespective of the PVA nature, denoting a slower erosion mechanism (see Figure S5). Finally, for all samples prepared with a total PVA content of 7.5 w/v %, no significant scattering was observed and the carriers remained stable toward erosion/dissolution, indicating a strictly diffusive release of the probe from the swelled carriers, as observed in the monolithic carriers. The behavior of the evaluated pellets is summarized in Figure 7.

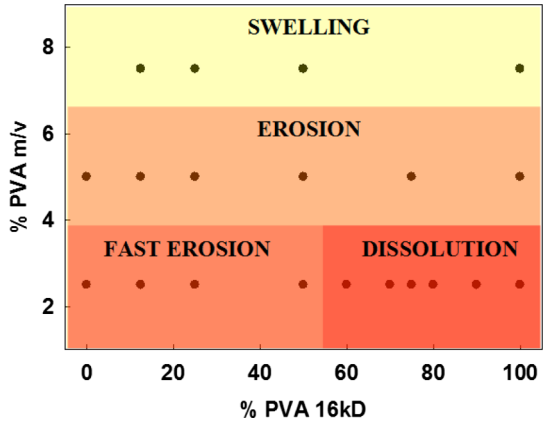

Figure 7. Stability behavior of the pellets as a function of total PVA content and formulation.

CONCLUSIONS

The controlled ice templating of aqueous solutions containing mixtures of PVA and the subsequent freeze-drying can be adapted to the preparation of molecular carriers with a range of dimensions and textures, ranging from monolithic large pieces to millimetric pellets. If the carriers are prepared from solutions composed of mixtures of PVA of different molecular weights, intimate polymer mixtures result, resulting in physical properties that stand in between those of the bare end members.

Monolithic carriers are stable in aqueous solution, and the probe release is governed by a swelling−diffusion mechanism. The kinetics of the probe release can be delayed from minutes to hours with increasing total PVA content, the average PVA molecular weight, or the relative composition, in the case of binary PVA mixtures. However, the tendency is far from being easy to predict, and an extensive screening is mandatory.

In the case of pellets (millimetric carriers), the probe release is restricted to the scale of minutes, irrespective of the PVA content or composition. However, the content and nature of PVA dramatically affect the stability of the polymeric matrix immersed in water. Depending on the formulation, the carriers can develop swelling, erosion or eventually massive dissolution.

EXPERIMENTAL SECTION

Materials and Chemicals. *Sample Preparation.* Solutions of PVA of 16 kD average molecular weight (98% of hydrolysis) and/or 90 kD average molecular weight (>99% of hydrolysis) were prepared in deionized water. The total concentration of PVA was varied in the range 2.5−10% by weight in volume; samples were denoted *X*L*Y*% with *X* representing the total weight/volume percentage of PVA in the parent solution and *Y* % representing the mass percentage of low-molecular-weight PVA (16 kD) with respect to the total polymer mass (PVA 16 kD + PVA 90 kD). All PVA samples prepared for release determinations were also loaded with methyl orange probe (0.25% weight in dry PVA weight basis).

Ice Structuration. *Monoliths.* Samples with controlled freezing rate and oriented gradient were prepared by loading PVA solutions into the molds, typically insulin syringes (length 80 mm and diameter 4 mm) and subsequently directionally frozen by dipping the molds at defined rates into a −196 °C (liquid nitrogen) cold bath. Because the ice-front progress state reached a stationary value (e.g., nominal) at the upper half of the sample, the characterization and experiments were always conducted on that portion of the monolith.[26]

Pellets. Isotropically flash-frozen spheroids were prepared by dropping the aforementioned PVA solutions into the liquid nitrogen cold bath. For each sample formulation, several pellets were prepared for release experiments. A couple of pellets were fractured to exhibit the inner structural features.

Both frozen pellets and monoliths were submitted to lyophilization using an Alpha 1-2 LD Plus freeze-drier; the resulting scaffolds were kept at room temperature in a desiccator for further characterization.

Physical and Morphological Characterization. The microstructures of the obtained monolith scaffolds were observed by SEM (Zeiss SUPRA 40). Pore dimension and wall thickness of the monoliths were determined from SEM micrographs of cross sections to the direction of freezing. The crystallinity and thermal stability of representative bare PVA samples prepared without the addition of methyl orange were explored. PXRD was recorded measuring the samples from 5 to 60°, with a 0.02° step size and a 1 s step time. DSC (Shimadzu DSC 50) of samples (3−5 mg) sealed in 40 μL Al crucible pans was recorded from 25 to 300 °C at 5 °C min^{-1} under a nitrogen atmosphere.

Stability and Release Characterization. Release experiments were carried out by the straight immersion of 10 mg of carrier in 10 mL of water under permanent stirring, preventing the straight contact of the magnetic bar with the PVA matrix, to avoid mechanical disruption. The cumulative release of the dye was determined by measuring the absorbance of the liquid phase at 464 nm with recycling aliquots by maintaining the volume constant throughout the experiment. For samples that

DOI: 10.1021/acsomega.7b01961
ACS Omega 2018, 3, 2390−2395

evidenced erosion and/or dissolution, the scattering signal of PVA particles was deduced by subtracting the contribution of the molecular spectrum of the released probe recorded from the total absorbance signal.

■ ASSOCIATED CONTENT

Supporting Information

The Supporting Information is available free of charge on the ACS Publications website at DOI: 10.1021/acsomega.7b01961.

Magnified FESEM images, PXRD patterns, and scattering thresholds (PDF)

■ AUTHOR INFORMATION

Corresponding Author

*E-mail: jobbag@qi.fcen.uba.ar.

ORCID

Matías Jobbágy: 0000-0002-6860-341X

Notes

The authors declare no competing financial interest.

■ ACKNOWLEDGMENTS

This work was supported by the University of Buenos Aires (UBACyT 20020130100610BA), the Agencia Nacional de Promoción Científica y Tecnológica (ANPCyT PICT 2012-1167), and the National Research Council of Argentina (CONICET PIP 11220110101020). J.M.S. acknowledges CONICET for postdoctoral fellowship; J.M.F.-C. thanks COLCIENCIAS for the doctoral scholarship. J.M.S. and M.J. are Research Scientists of CONICET (Argentina).

■ REFERENCES

(1) Hollister, S. J. Porous scaffold design for tissue engineering. *Nat. Mater.* **2005**, *4*, 518−524.

(2) Rezwan, K.; Chen, Q. Z.; Blaker, J. J.; Boccaccini, A. R. Biodegradable and bioactive porous polymer/inorganic composite scaffolds for bone tissue engineering. *Biomaterials* **2006**, *27*, 3413−3431.

(3) Jones, J. R.; Ehrenfried, L. M.; Hench, L. L. Optimising bioactive glass scaffolds for bone tissue engineering. *Biomaterials* **2006**, *27*, 964−973.

(4) Ohtsuki, C.; Kokubo, T.; Yamamuro, T. Mechanism of Apatite Formation on CaOSiO2P2O5 Glasses in a Simulated Body Fluid. *J. Non-Cryst. Solids* **1992**, *143*, 84−92.

(5) Kokubo, T.; Kim, H.-M.; Kawashita, M. Novel bioactive materials with different mechanical properties. *Biomaterials* **2003**, *24*, 2161−2175.

(6) Minaberry, Y.; Jobbágy, M. Macroporous Bioglass Scaffolds Prepared by Coupling Sol-Gel with Freeze Drying. *Chem. Mater.* **2011**, *23*, 2327−2332.

(7) Onna, D.; Minaberry, Y.; Jobbágy, M. Hierarchical bioglass scaffolds: Introducing the "milky way" for templated bioceramics. *J. Mater. Chem. B* **2015**, *3*, 2971−2977.

(8) Alves, M.-H.; Jensen, B. E. B.; Smith, A. A. A.; Zelikin, A. N. Poly(vinyl alcohol) physical hydrogels: New vista on a long serving biomaterial. *Macromol. Biosci.* **2011**, *11*, 1293−1313.

(9) Hassan, C. M.; Peppas, N. A. Structure and applications of poly(vinyl alcohol) hydrogels produced by conventional crosslinking or by freezing/thawing methods. *Advances in Polymer Science*; Springer, 2000; Vol. *153*, pp 37−65.

(10) Lozinsky, V. I.; Galaev, I. Y.; Plieva, F. M.; Savina, I. N.; Jungvid, H.; Mattiasson, B. Polymeric cryogels as promising materials of biotechnological interest. *Trends Biotechnol.* **2003**, *21*, 445−451.

(11) Gutiérrez, M. C.; Ferrer, M. L.; del Monte, F. Ice-templated materials: Sophisticated structures exhibiting enhanced functionalities obtained after unidirectional freezing and ice-segregation-induced self-assembly. *Chem. Mater.* **2008**, *20*, 634−648.

(12) Ferrer, M. L.; Esquembre, R.; Ortega, I.; Reyes Mateo, C.; Del Monte, F. Freezing of binary colloidal systems for the formation of hierarchy assemblies. *Chem. Mater.* **2006**, *18*, 554−559.

(13) Gutiérrez, M. C.; García-Carvajal, Z. Y.; Jobbágy, M.; Rubio, F.; Yuste, L.; Rojo, F.; Ferrer, M. L.; del Monte, F. Poly(vinyl alcohol) scaffolds with tailored morphologies for drug delivery and controlled release. *Adv. Funct. Mater.* **2007**, *17*, 3505−3513.

(14) Gutiérrez, M. C.; García-Carvajal, Z. Y.; Jobbágy, M.; Yuste, L.; Rojo, F.; Abrusci, C.; Catalina, F.; del Monte, F.; Ferrer, M. L. Hydrogel scaffolds with immobilized bacteria for 3D cultures. *Chem. Mater.* **2007**, *19*, 1968−1973.

(15) Aranaz, I.; Gutiérrez, M. C.; Yuste, L.; Rojo, F.; Ferrer, M. L.; del Monte, F. Controlled formation of the anhydrous polymorph of ciprofloxacin crystals embedded within chitosan scaffolds: Study of the kinetic release dependence on crystal size. *J. Mater. Chem.* **2009**, *19*, 1576−1582.

(16) Minaberry, Y.; Chiappetta, D. A.; Sosnik, A.; Jobbágy, M. Micro/nanostructured hyaluronic acid matrices with tuned swelling and drug release properties. *Biomacromolecules* **2013**, *14*, 1−9.

(17) Deville, S. Ice-templating, freeze casting: Beyond materials processing. *J. Mater. Res.* **2013**, *28*, 2202−2219.

(18) Zhang, H.; Hussain, I.; Brust, M.; Butler, M. F.; Rannard, S. P.; Cooper, A. I. Aligned two- and three-dimensional structures by directional freezing of polymers and nanoparticles. *Nat. Mater.* **2005**, *4*, 787−793.

(19) Deville, S.; Maire, E.; Bernard-Granger, G.; Lasalle, A.; Bogner, A.; Gauthier, C.; Leloup, J.; Guizard, C. Metastable and unstable cellular solidification of colloidal suspensions. *Nat. Mater.* **2009**, *8*, 966−972.

(20) Thomas, D.; Cebe, P. Self-nucleation and crystallization of polyvinyl alcohol. *J. Therm. Anal. Calorim.* **2017**, *127*, 885−894.

(21) Korsmeyer, R. W.; Gurny, R.; Doelker, E.; Buri, P.; Peppas, N. A. Mechanisms of Solute Release from Porous Hydrophilic Polymers. *Int. J. Pharm.* **1983**, *15*, 25−35.

(22) Korsmeyer, R. W.; Peppas, N. A. Effect of the Morphology of Hydrophilic Polymeric Matrices on the Diffusion and Release of Water Soluble Drugs. *J. Membr. Sci.* **1981**, *9*, 211−227.

(23) González, B.; Colilla, M.; Vallet-Regí, M. Time-delayed release of bioencapsulates: A novel controlled delivery concept for bone implant technologies. *Chem. Mater.* **2008**, *20*, 4826−4834.

(24) Kim, H.; Fassihi, R. Application of binary polymer system in drug release rate modulation. 2. Influence of formulation variables and hydrodynamic conditions on release kinetics. *J. Pharm. Sci.* **1997**, *86*, 323−328.

(25) Pillay, V.; Fassihi, R. In vitro release modulation from crosslinked pellets for site-specific drug delivery to the gastrointestinal tract: I. Comparison of pH-responsive drug release and associated kinetics. *J. Controlled Release* **1999**, *59*, 229−242.

(26) Deville, S.; Saiz, E.; Tomsia, A. P. Ice-templated porous alumina structures. *Acta Mater.* **2007**, *55*, 1965−1974.

DOI: 10.1021/acsomega.7b01961
ACS Omega 2018, 3, 2390−2395